

Bifurcation in Asymmetrically Coupled BVP Oscillators

Tetsushi Ueta* and Hiroshi Kawakami

October 23, 2002

Abstract

BVP oscillator is the simplest mathematical model describing dynamical behavior of the neural activity. The large scale neural network can often be described naturally by coupled systems of BVP oscillators. However, even if two BVP oscillators are merely coupled by a linear element, the whole system exhibits complicated behavior. In this letter, we analyze a coupled BVP oscillators with asymmetrical coupling structure, besides, each oscillator has different internal resistance. The system shows a rich variety of bifurcation phenomena, and strange attractors. We calculate bifurcation diagrams in 2-parameter plane around which the chaotic attractors mainly appears and confirm relaxant phenomena in the laboratory experiments. We also briefly report a conspicuous strange attractor.

Keywords: BVP oscillator, bifurcation, chaos

1 Notation

- h Hopf bifurcation of an equilibrium
- I^k period-doubling bifurcation of a limit cycle with period- k
- G tangent bifurcation of a limit cycle
- Pf pitchfork bifurcation of a limit cycle

2 Introduction

At the first time, BVP (Bonhöffer van der Pol) equation has been derived as a simplified model of Hodgkin-Huxley (abbr. HH) equation by FitzHugh and Nagumo. They reduce the HH equation (four-dimensional) to a two-dimensional system called the BVP equation or FitzHugh-Nagumo model by extracting excitability of the dynamics of the dynamic behavior in the HH equation. The BVP equation, as the reduced model, can be regarded as a reasonable extension of van der Pol equation. In fact, the BVP equation can be realized by a circuitry by using simple passive elements and one nonlinear conductor. Nowadays the BVP equation becomes one of classic nonlinear

*This work partially supported by Grant-in-Aid for Encouragement of Young Scientists 12750365, Japan Society for the Promotion of Science.

oscillator models and it has been studied for last 2 decades. As applications of the BVP equation under above background, bifurcation structures and classification of synchronization phenomena in the resistively coupled BVP oscillators have been studied[Papy *et al.*, 1995, Papy *et al.*, 1996, Kitajima *et al.*, 1998]. They focused only on the behavior of the coupled system consisting of ‘identical’ oscillators (all oscillators have same parameter values). It enables us to analyze the system in symmetry point of view by using group theory. To investigate such coupled system, identical oscillators are chosen as an oscillator unit since mathematical properties of symmetry can reduce the bifurcation problem about equilibria and periodic solutions. However, in the previous work[Ueta *et al.*, 2001], we found out that a coupled system with ‘unbalanced’ oscillator can behave complex, i.e., typical local bifurcations are only caused in such unbalanced coupled situation.

In this letter, we investigate the asymmetrically coupled BVP oscillators. We focus our eyes on ‘unbalanced’ situation in the coupled system, namely, two BVP oscillators are coupled, and each of them has different value of the internal impedance. Then we found an odd shape of chaotic attractor after the period-doubling bifurcation cascade. This result points out that the coupling system of identical oscillators does not have a rich variety of nonlinear phenomena with a reasonable parameter range.

3 Asymmetrical coupled BVP oscillators.

Figure 1 shows an asymmetrically coupled BVP oscillators. The nonlinear negative conductance is modeled by

$$g(v) = -a \tanh bv. \quad (1)$$

From physical measurement of FET, we can directly determine parameter values:

$$a = 6.89 \times 10^{-3}, \quad b = 0.3523.$$

We also fix parameters as

$$L = 10[\text{mH}], \quad C = 0.022[\mu\text{F}].$$

Then the natural frequency of the LC tank is

$$Z_0 = \sqrt{L/C} = 674.19986[\Omega].$$

Then we have the following circuit equations:

$$\begin{aligned} C \frac{dv_1}{dt} &= -i_1 - g(v_1) \\ L \frac{di_1}{dt} &= v_1 - r_1 i_1 + \frac{Gr_1}{1+Gr_1} (r_1 i_1 - v_2) \\ C \frac{dv_2}{dt} &= -i_2 - g(v_2) + \frac{G}{1+Gr_1} (r_1 i_1 - v_2) \\ L \frac{di_2}{dt} &= v_2 - r_2 i_2 \end{aligned} \quad (2)$$

where, $G = 1/R$. Now we choose the following transformations:

$$\begin{aligned} x_j &= \frac{v_j}{a} \sqrt{\frac{C}{L}}, & y_j &= \frac{i_j}{a}, & k_j &= r_j \sqrt{\frac{C}{L}}, & j &= 1, 2. \\ \tau &= \frac{1}{\sqrt{LC}} t, & \gamma &= ab \sqrt{\frac{L}{C}}, & \delta &= G \sqrt{\frac{L}{C}}, & \eta &= \frac{1}{1 + \delta k_1} \end{aligned}$$

hence we have normalized differential equations as follows:

$$\begin{aligned} \dot{x}_1 &= -y_1 + \tanh \gamma x_1 \\ \dot{y}_1 &= x_1 - k_1 y_1 + \delta k_1 \eta (k_1 y_1 - x_2) \\ \dot{x}_2 &= -y_2 + \tanh \gamma x_2 + \delta \eta (k_1 y_1 - x_2) \\ \dot{y}_2 &= x_2 - k_2 y_2. \end{aligned} \tag{3}$$

Notice that $\delta \rightarrow 0$ means decoupling of oscillators.

This equation has a symmetry such that

$$\begin{aligned} P : \mathbf{R}^4 &\rightarrow \mathbf{R}^4 \\ (x_1, y_1, x_2, y_2) &\mapsto (-x_1, -y_1, -x_2, -y_2). \end{aligned} \tag{4}$$

This fact directly affects the structure of the state space, namely, if there exists a periodic solution $\varphi(t) \in \mathbf{R}^4$, then $-\varphi(t)$ also forms a periodic solution. Besides the pitchfork bifurcation is possibly caused by this symmetrical property.

To solve bifurcation problem for attractors in Eq. (3), we use Newton's method and Poincaré mapping. The latter reduces the continuous-time system into discrete one, and enables us to analyze topological properties of periodic solutions. The shooting method like continuation[?] and its improved method[Ueta, *et al.*, 1997] are used.

4 Bifurcations in k_1 - k_2 Plane

To show a rich variety of complex behavior in Eq.3, we firstly fix the coupling coefficient δ as $Z_0/1000 = 0.674$ ($R = 1000[\Omega]$). In this case, variable parameters are k_1 and k_2 (according to variable resistances r_1 and r_2). Figure 2 shows a bifurcation diagram.

Basically the limit cycle is caused by a supercritical Hopf bifurcation of the origin (not shown this diagram). While, two unstable equilibria $C^+ = (x_{1c}, y_{1c}, x_{2c}, y_{2c})$, $C^- = (-x_{1c}, -y_{1c}, -x_{2c}, -y_{2c})$ are generated by the pitchfork bifurcation. Besides they are changed to be stable via the subcritical Hopf bifurcation h , then an unstable limit cycle is generated. These stable and unstable limit cycles are disappeared by the tangent bifurcation curves G . Thus the whole parameter plane is split into two parts, oscillatory (shaded) and non-oscillatory (white) areas, which are edged by G and h . In non-oscillatory region, the orbit with any initial condition is eventually attracted by C^+ or C^- .

The lower figure of Fig. 2 is an enlargement diagram extracted from the oscillatory region. We explain bifurcation phenomena along points from (a) to (d), which are shown in this figure. At point (a), there exist a stable limit cycle. Pf is the pitchfork bifurcation of a limit cycle, and then

stable two limit cycles are generated. Figure 3(c) shows one of limit cycles just after the pitchfork bifurcation. (another stable limit cycle is obtained by using an initial state from a property Eq. (4)). These cycles would be bifurcated by period-doubling bifurcation I . Period 2^k cycles are successively generated via period-doubling cascade along the direction of arrows in the figure. Eventually chaotic attractor is obtained, see Fig 3(d). It is difficult show period-doubling cascade by I^k because the bifurcation process goes rapidly with slightly changed parameter values along the arrows. The chaotic attractor forms a double scroll and finally disappeared by reaching Hopf bifurcation h , i.e., the orbit around C^\pm stays the point forever after this bifurcation. Note that the limit cycle before getting pitchfork bifurcation (Fig. 3(a) and (b)) is never met period-doubling bifurcation. Only the asymmetric limit cycle (Fig.3(c)) can be bifurcated as period-doubling.

5 Bifurcations in δ - k_2 Plane

We choose one of the parameters as $k_2 = 1.05$. In this parameter value, the system behave moderate with variation of k_1 with fixed δ mentioned above. However, the following results show that the system motion also becomes complex in δ - k_2 plane.

Figure 4 is a bifurcation diagram in δ - k_2 plane. In global area, a similar bifurcation structure described in the previous section is observed, however, inside peninsula of the tangent bifurcation G , a clear period-doubling cascade labeled by I^k can be visualized. Figures 5 (a)–(c) are corresponding attractors. The pitchfork bifurcation also plays important role to generate double scroll, namely, the limit cycle rotating about the origin is destabilized by this bifurcation. This can form a channel between two Rössler type chaos attractors about C^\pm . Figure 5 (d) shows a double scroll attractor.

Figure 7 shows all Lyapunov exponent for the attractor by changing parameter δ along $k_2 = 1.05$. Typical period-doubling cascade is recognized, and the positive Lyapunov exponent is an evidence of chaotic behavior. In $\delta \approx 1.89$, the second exponent also shows small positive value, however, under this parameter value, the chaotic attractor stays comparatively long around two unstable equilibria C^\pm . We have chosen $x_1 = 0$ as the Poincaré section to evaluate exponents of a double scroll attractor fairly, but rather this choice causes unfair evaluation of exponent in this parameter value, that is, the orbit transverses the Poncaré section very few. Thus the result near this parameter value is not reliable, and we have to prepare another evaluation method for this case in future.

6 Laboratory Experiments and Bursting Phenomenon

Since the model equation of the FET is sufficiently accurate for low frequency of LC tank, all dynamical behavior investigated above can be realized in an electrical circuitry. Figure 8 illustrates the period-doubling cascade and chaotic behavior corresponding to Fig. 5 as R is decreased.

For other choice of parameter values, we noticed that there is a conspicuous bursting response. Figure 9 visualize a spatio-temporal pattern of a chaotic motion, i.e., the orbit is wandering between a double scroll and an unstable limit cycle even the circuit (2) is only a four-dimensional system. To analyze this attractor would be a future problem.

7 Conclusions

In this letter, we analyzed a asymmetrically coupled BVP oscillators. Each oscillator has different internal resistance, i.e., two different rhythms are coupled by a register. We showed bifurcation diagrams of equilibria and periodic solutions and confirmed relaxant phenomena in the laboratory experiments. The spatio-temporal (switching) behavior that the state wandering two chaotic attractors alternatively is found.

Acknowledgement

The authors wish to thank Mrs. H. Wagi for her calculation results.

References

- [Kitajima *et al.*, 1998] Kitajima, H., Katsuta, Y., Kawakami, H. [1998] “Bifurcations of periodic solutions in a coupled oscillator with voltage ports,” *IEICE Trans. Fundamentals*, **E81-A**, pp.476-482, 1998.
- [Papy *et al.*, 1995] Papy, O., and Kawakami, H. [1995] “Symmetrical properties and bifurcations of the periodic solutions for a hybridly coupled oscillator,” *IEICE Trans. Fundamentals*, **E78-A**, 1816–1821, 1995.
- [Papy *et al.*, 1996] Papy, O., Kawakami, H. [1996] “Symmetry breaking and recovering in a system of n hybridly coupled oscillators,” *IEICE Trans.* **E79-A**, 1581-1586, 1996.
- [Ueta *et al.*, 2001] Ueta, T., Kousaka, T., Kawakami, H. [2001] “Strange attractor in resistively coupled BVP oscillators,” In *Proc. 2001 Int. Conf. on Progress in Nonlinear Science*, Nizhny Novgorod, Russia, July 2001. (in press)
- [Ueta, *et al.*, 1997] Ueta, T., Tsueike, M., Kawakami, H., Yoshinaga, T., Katsuta, Y. [1997] “A computation of bifurcation parameter values for limit cycles,” *IEICE Trans. Fundamentals*, **E80-A**, 1725–1728, 1997.

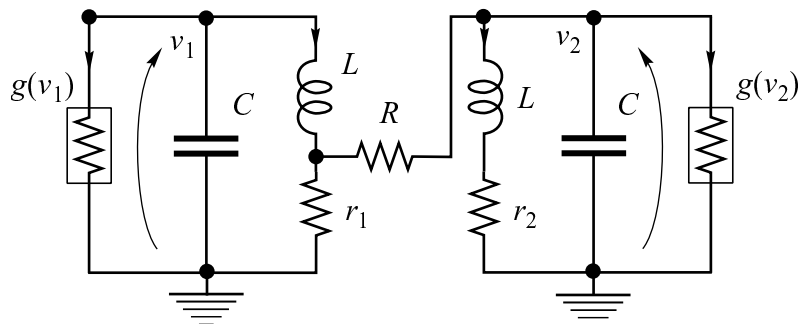
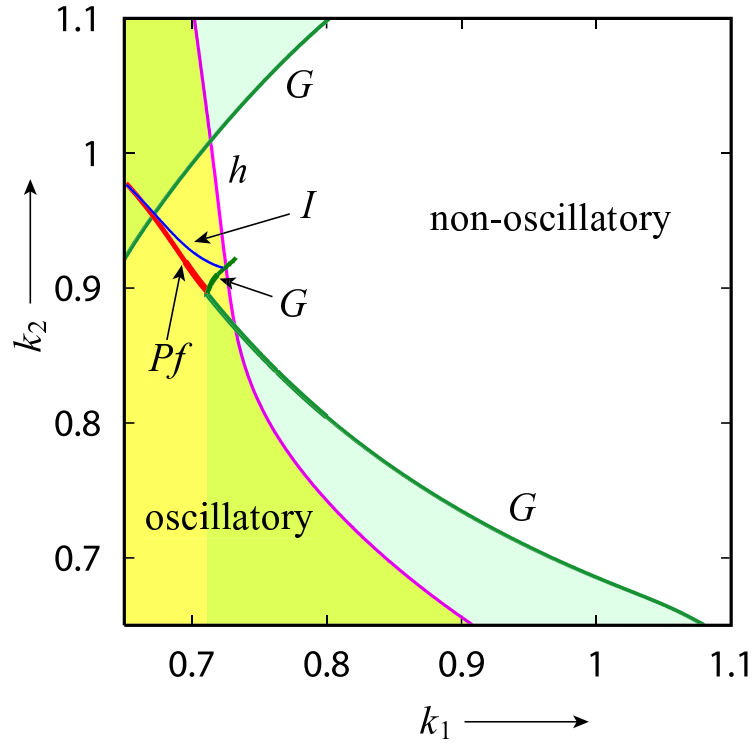
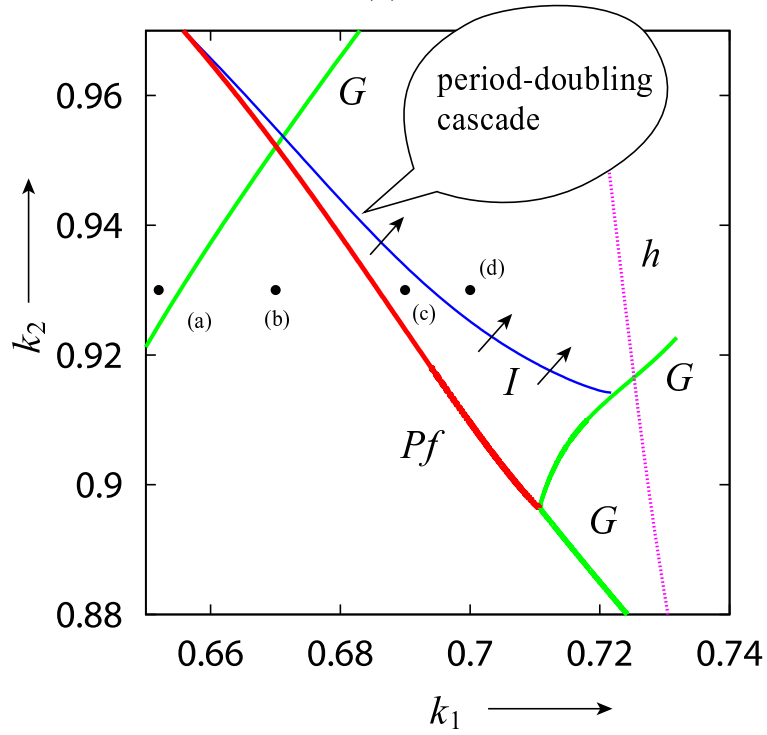


Figure 1: Asymmetrical Coupled BVP Oscillators



(a)



(b)

Figure 2: Bifurcation diagram of equilibria and periodic solutions of Eq. (3) in k_1 - k_2 plane. (a): global area, (b): enlargement of (a).

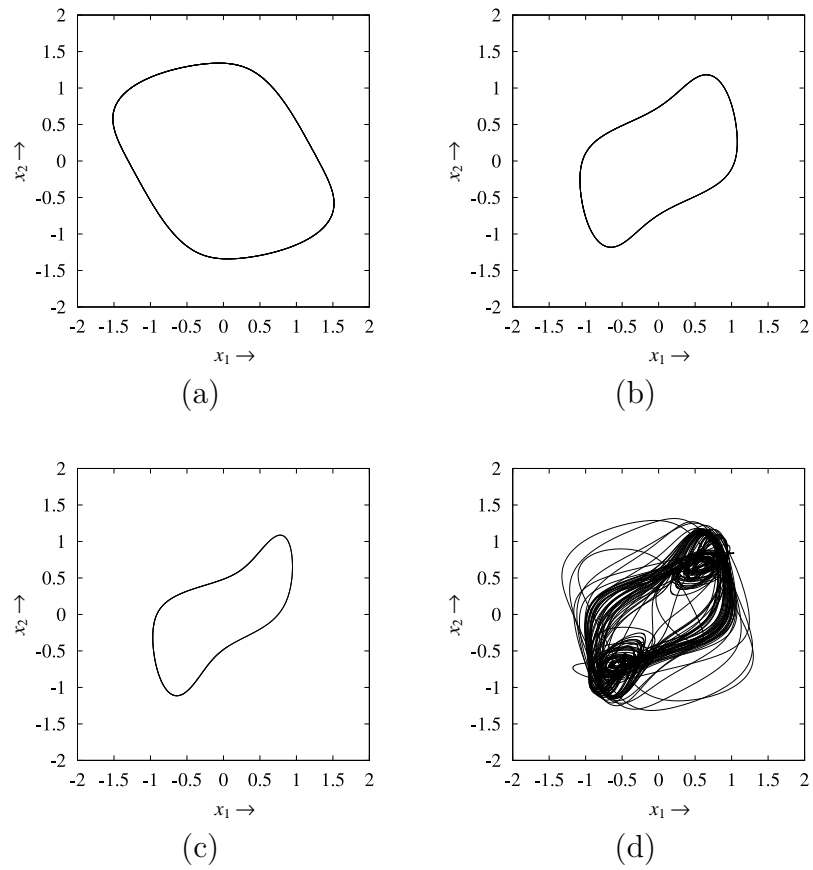


Figure 3: Phase portraits (projections into x_1 - x_2 plane) corresponding to the points (a)–(d) marked in Fig. 2(b). $k_2 = 0.93$. (a): $k_1 = 0.652$, (b): $k_1 = 0.67$, (c): $k_1 = 0.69$, (d): $k_1 = 0.70$,

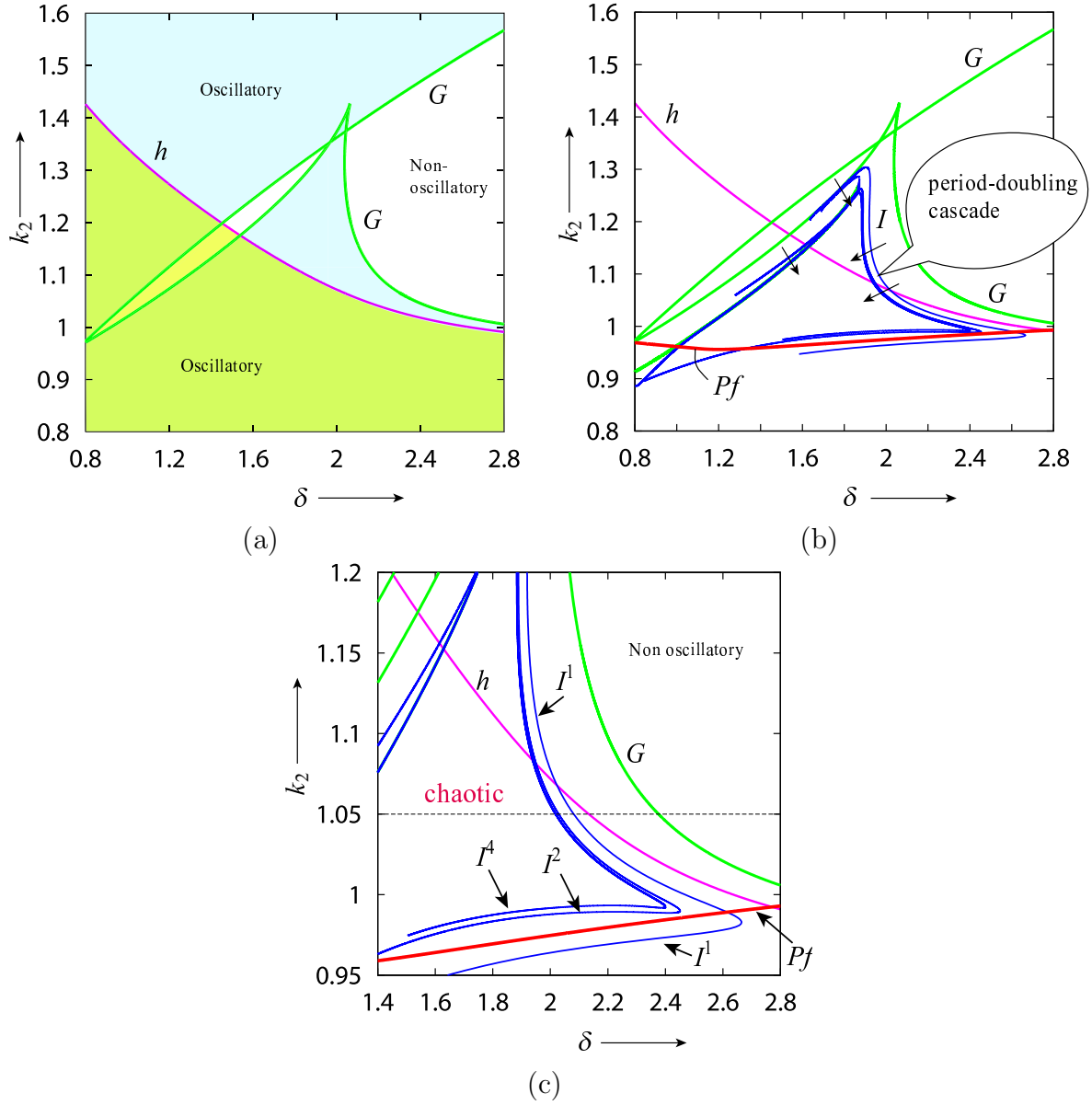


Figure 4: Bifurcation diagram of equilibria and periodic solutions of Eq.(3) in δ - k_2 plane. $k_1 = 0.653$. (a): global area, (b): bifurcation structure in detail. (c): enlargement of (b).

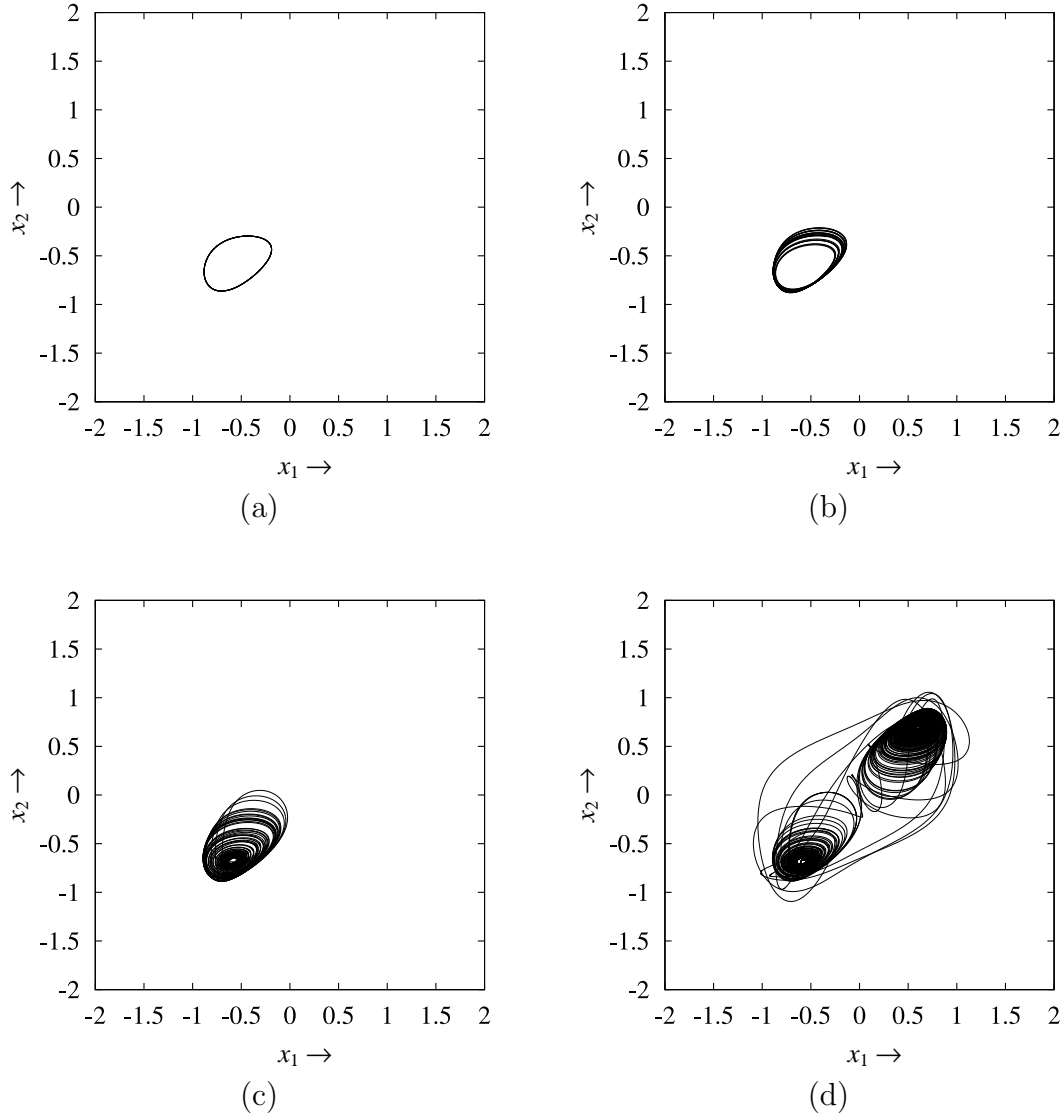


Figure 5: Phase portraits (projections into x_1 - x_2 plane) with $k_2 = 1.05$. (a): $\delta = 2.10$, (b): $\delta = 2.00$, (c): $\delta = 1.90$, (d): $\delta = 1.88$.

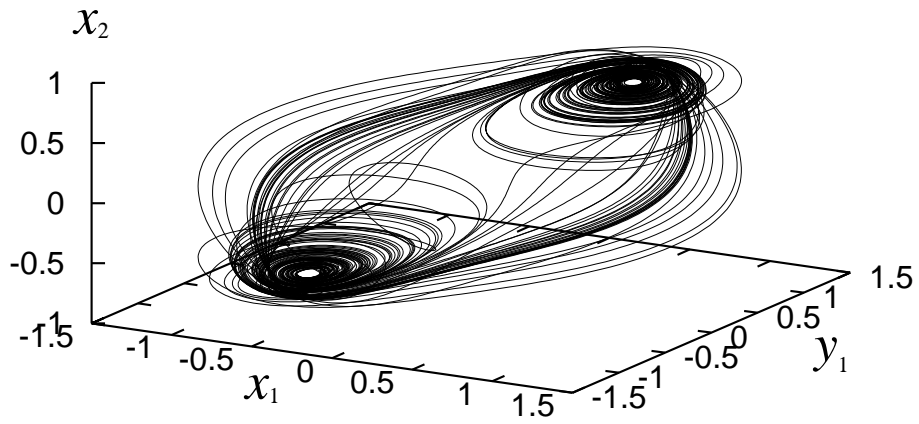


Figure 6: 3D $(x_1-x_2-y_1)$ projection of the strange attractor. $k_1 = 0.653$, $k_2 = 1.05$, $\delta = 1.4$

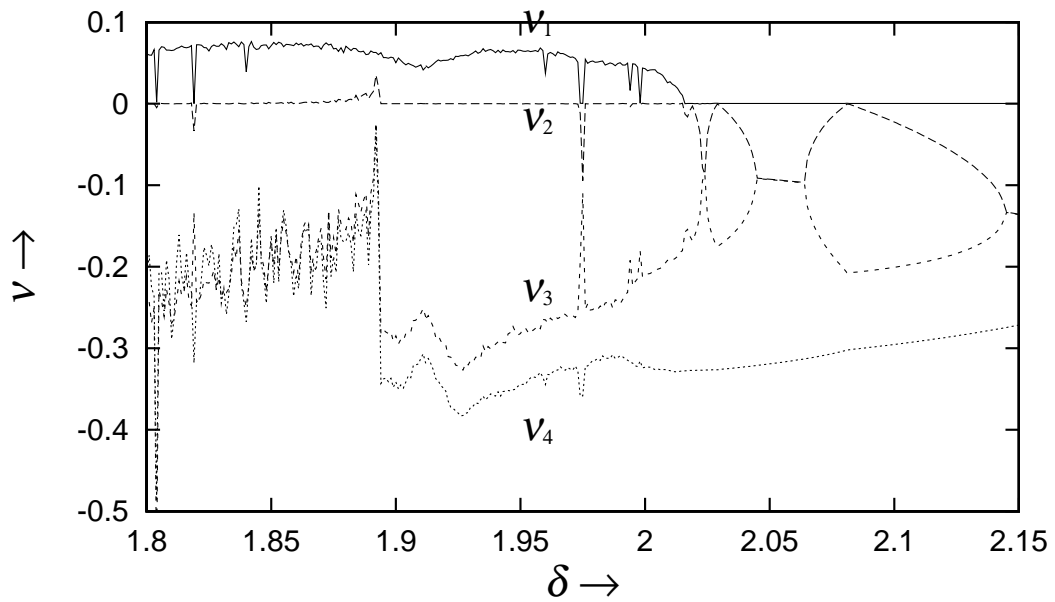


Figure 7: Lyapunov exponents. $k_2 = 1.05$.

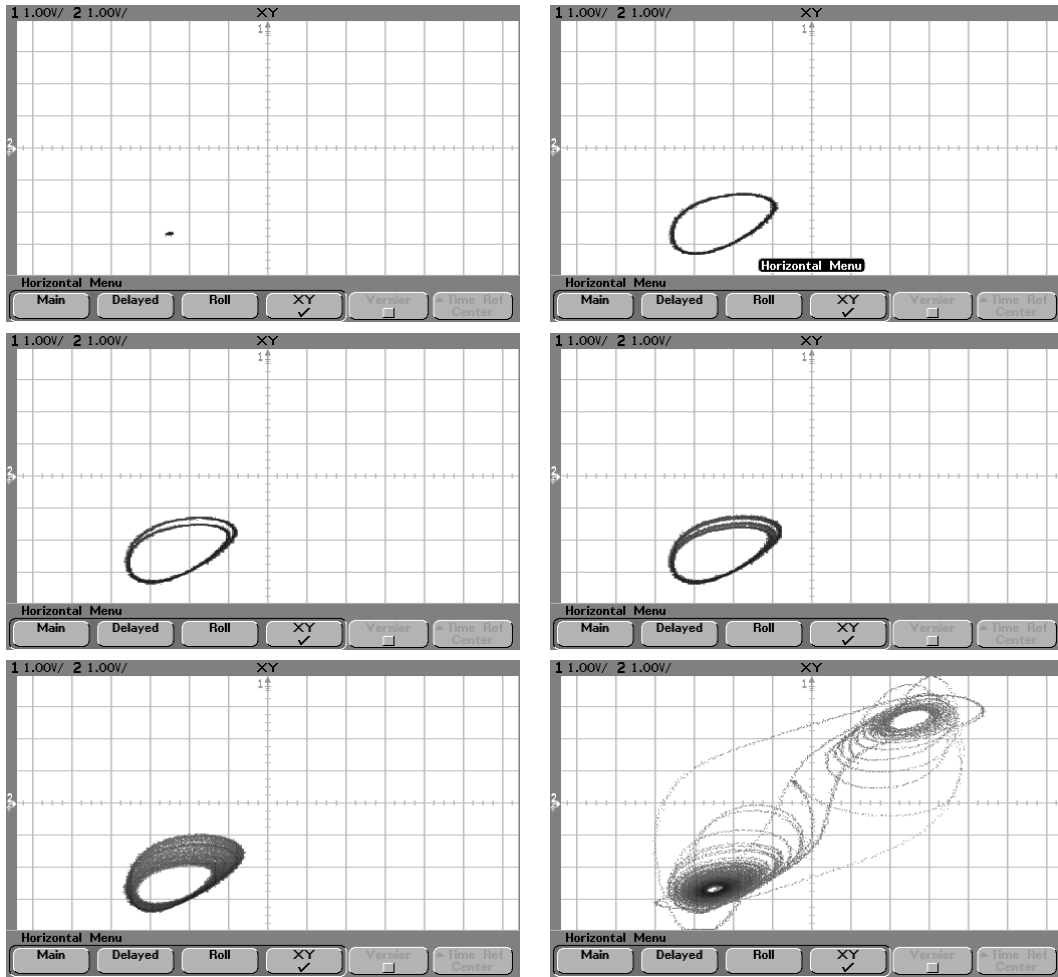
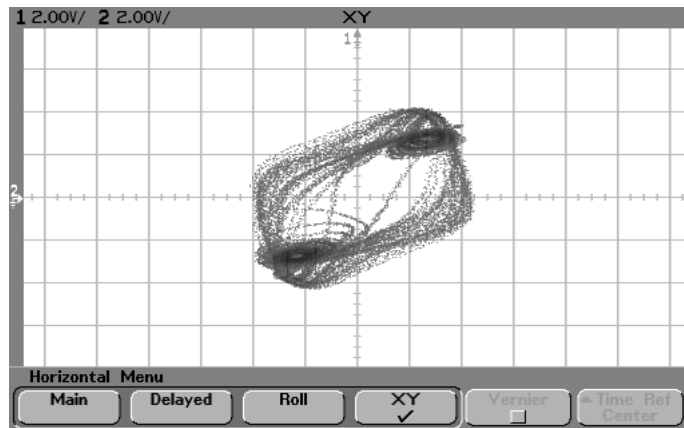
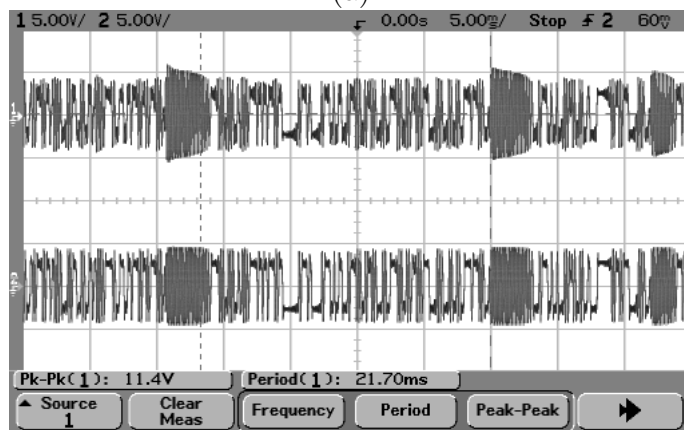


Figure 8: Laboratory experiments according to Fig.5, v_1-v_2 , 2[V/dev].



(a)



(b)

Figure 9: Bursting response. $R = 1.6[\text{K}\Omega]$. The transient state wanders around an unstable periodic solution and a double scroll. (a): phase portrait. v_1 - v_2 . 2[V/dev]. (b): snapshot of the time response. Upper: v_1 , Lower: v_2 . Abscissa 5 msec/dev, ordinate 5[V/dev].,